KALMAN FILTER BASED ESTIMATION OF NEUTRAL-AXIS POSITION OF BRIDGE DECK SECTIONS USING STRAIN MONITORING DATA

Y.Q. Ni* and H.W. Xia
Department of Civil and Environmental Engineering, The Hong Kong Polytechnic University,
Hung Hom, Kowloon, Hong Kong. *Email: ceyqni@polyu.edu.hk

ABSTRACT

The neutral-axis position has been recognized as a damage indicator for bridge deck assessment because of its high sensitivity to local damage on deck sections. It can be estimated when strain responses at the top and bottom of a deck cross-section under traffic loading are measured. However, the accuracy of neutral-axis position estimation directly using the measured strain responses might be significantly distorted in the presence of measurement noise and varying traffic load patterns. In this study, a Kalman filter (KF) estimator is formulated to locate the neutral-axis position from measured strain responses under traffic loading. Its capability for consistently locating the neutral-axis position under varying traffic load patterns is verified using the field monitoring data of traffic-induced strain responses acquired from the suspension Tsing Ma Bridge under diverse load scenarios (highway traffic, railway traffic, and their combination). The results indicate that the proposed KF estimator gives rise to consistent neutral-axis position estimation results which are independent of load conditions and patterns.

KEYWORDS

Bridge deck, structural health monitoring, neutral-axis position, strain measurement, Kalman filter based estimation.

INTRODUCTION

In-service bridge structures are subject to age-related deterioration, service demands for increasing traffic flow and heavier truck loads, natural or man-made disasters, leading to concerns regarding the safety and serviceability of the bridges. Continuous awareness of the evolution of the structural condition of in-service bridge structures is of great value for their owners as it allows making informed decisions on the maintenance and management of the infrastructure assets. Long-term structural health monitoring (SHM), on a continuous basis, provides plentiful information regarding structural behavior by various sensors and traces the health status of existing structures in a real-time way so that early warnings could be signaled before catastrophic failure happens (Aktan *et al*. 2001; Mufti 2002; Ko and Ni 2005; Fujino *et al*. 2009; Ni *et al*. 2011).

Real-time monitoring of strain is emerging as a critical strategy in the assessment, inspection and decision making on maintenance/repair of bridge structures (Catbas and Aktan 2002; Chakraborty and DeWolf 2006; Adewuyi *et al*. 2009; Liu *et al*. 2009; Wang and Yim 2010; Ni *et al*. 2012; Xia *et al*. 2012). Strain data can be directly used to indicate the safety reserve of a bridge component or provide information on the load-carrying capacity of the whole bridge; they would be better suited to characterize local damage of a bridge than vibration data when strain gauges are appropriately deployed. The limitation on the spatial resolution of strain measurement using conventional strain gauges (vibrating-wire type and electrical-resistant type) is being broken down by the development of distributed fiber Bragg grating (FBG) and Brillouin optical fiber (BOF) sensing techniques (Li *et al*. 2004; Bastianini *et al*. 2007; Glišić and Inaudi 2007; Wu *et al*. 2008; Ansari 2009; Bao and Chen 2011).

Bridge deck that directly carries traffic load is one of the most critical parts of a bridge system. Deterioration of bridge deck can cause public inconvenience, travel delay, economic impact, and even life lost, giving rise to the most severe problem for the highway industry today. For example, the deck trusses of the I-35W Bridge over the Mississippi River in Minneapolis, Minnesota, USA collapsed on August 1, 2007 without warning (NTSB 2008). As a result of the catastrophic failure, 13 people died and 145 people were injured. This accident highlights again the importance of incorporating structural monitoring technologies into current bridge management programs to prevent similar tragedies in the future. In selecting monitoring-based indices for bridge deck condition assessment, their sensitivity to damage and robustness with respect to random traffic load patterns are two main factors of concern.

The neutral-axis position of bridge deck sections has been proposed as a damage indicator for bridge deck assessment because it reflects the local cross-section property and shifts when damage on the deck cross-section occurs (Chakraborty and DeWolf 2006; Cardini and DeWolf 2009; Xia 2011). Although the strain responses at different points of a deck cross-section under varying traffic loading evolve with time, their ratio would keep constant in the absence of damage and it can be used to derive the neutral-axis position. It has been demonstrated that the strain-derived neutral-axis position is considerably sensitive to local damage on the deck (Xia 2011). However, the accuracy of neutral-axis position estimation directly using the measured strain data might be significantly distorted in the presence of measurement noise and varying traffic load patterns. In this study, a Kalman filter (KF) estimator is formulated to reliably locate the neutral-axis position from measured strain responses under traffic loading. Its capability for consistently locating the neutral-axis position under varying traffic load patterns is verified using the field monitoring data of traffic-induced strain responses from the instrumented Tsing Ma Bridge (TMB) which carries both highway and railway traffic.

NEUTRAL-AXIS POSITION AND KF ESTIMATOR

Direct Estimation of Neutral-axis Position

Beam-like bridge deck behaves like a flexural beam when traffic loads cause it to bend. According to the Euler-Bernoulli beam theory, the plane cross-sections of a bending beam remain plane after deformation and the strain distribution is linear over the depth of the cross-section. The strains at the bottom and top locations of the section are denoted by ε_b and ε_t, respectively, as shown in Figure 1. Following the geometric relation, the ratio of ε_b to ε_t can be expressed as

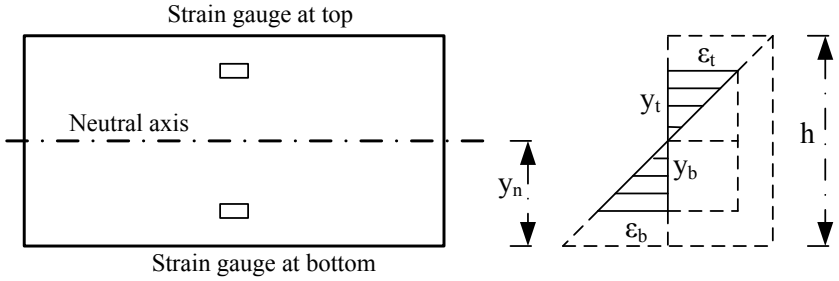

Figure 1 Flexural strain distribution on beam cross-section

$$\frac{\varepsilon_b}{\varepsilon_t} = \frac{y_b}{y_t} \tag{1}$$

where y_b is the distance between the bottom and the neutral axis; and y_t is the distance between the top and the neutral axis. From Eq. (1), we can obtain

$$\frac{\varepsilon_b}{\varepsilon_b + \varepsilon_t} = \frac{y_b}{y_b + y_t} = \frac{y_h}{h} \tag{2}$$

where y_n denotes the neutral-axis location of the cross-section; and h is the depth of the cross-section.

Eq. (2) relates the neutral-axis position in ratio (y_h/h) with the strains at the bottom and top of a cross-section. Under traffic loads, bending behavior dominates the response of beam-like bridge deck. When the strain responses at the top and bottom points are measured, the neutral-axis position can be estimated by

$$\hat{r} = \frac{\varepsilon_b}{\varepsilon_b + \varepsilon_t} \tag{3}$$

It is known (Xia 2011) that the efficiency of the above formula in estimating the neutral-axis position can be ensured only on condition that the measurement data are noise-free.

KF-based Estimation of Neutral-axis Position

The KF is purposed to use measurements observed over time (containing noise and other inaccuracies) to produce values that tend to be closer to the true values of the measurements (Kalman 1960; Brown and Hwang 1997). In this study, the neutral-axis position in ratio ($r = y_n/h$) is taken as the state variable to be estimated.

Because there is neither deterministic disturbance nor control scalar, the discrete model of the state in concern can be expressed by

$$r_k = \Phi_k r_{k-1} + w_k \tag{4}$$

where Φ_k is the propagation scalar that propagates the state from one sampling instant to the next; and w_k is the white process noise. The measurement equation is given as

$$z_k = H r_k + v_k \tag{5}$$

where H is the measurement scalar that relates the state to the observation z_k; and v_k is the measurement noise. The discrete KF equation for the system described by Eqs. (4) and (5) is

$$\hat{r}_k = \Phi_k \hat{r}_{k-1} + K_k (z_k - H\Phi_k \hat{r}_{k-1}) \tag{6}$$

and the error in the estimate can be expressed as

$$\tilde{r}_k = r_k - \hat{r}_k = r_k - \Phi_k \hat{r}_{k-1} - K_k (H r_k + v_k - H\Phi_k \hat{r}_{k-1}) \tag{7}$$

Noting that the state at time k can be replaced by an alternate expression at time k-1, it is obtained that

$$\tilde{r}_k = r_k - \hat{r}_k = r_k - \Phi_k \hat{r}_{k-1} - K_k (H\Phi_k r_{k-1} + H w_k + v_k - H\Phi_k \hat{r}_{k-1}) \tag{8}$$

or

$$\tilde{r}_k = (1 - K_k H)\tilde{r}_{k-1}\Phi_k + (1 - K_k H) w_k - K_k v_k \tag{9}$$

By squaring and then taking expectations of both sides of Eq. (9), we obtain the following covariance equation

$$P_k = (1 - K_k H)^2 M_k + K_k^2 R_k \tag{10}$$

where $P_k = E(\tilde{r}_k^2)$, $Q_k = E(w_k^2)$, $R_k = E(v_k^2)$, and $M_k = P_{k-1}\Phi_k^2 + Q_k$.

The KF gain K_k that minimizes the variance of the error in the estimate can be found by taking the derivative of Eq. (10) with respect to the gain and setting it equal to zero:

$$\frac{\partial P_k}{\partial K_k} = 2(1 - K_k H) M_k (-H) + 2 K_k R_k = 0 \tag{11}$$

Solving the above equation for the gain yields

$$K_k = \frac{M_k H}{H^2 M_k + R_k} = M_k H (H^2 M_k + R_k)^{-1} \tag{12}$$

Substitution of the optimal gain into the covariance equation gives

$$P_k = \frac{R_k K_k}{H} = \frac{M_k H - H^2 M_k K_k}{H} = M_k - H M_k K_k = 0 \tag{13}$$

or, more simply,

$$P_k = (1 - K_k H) M_k \tag{14}$$

The derivation given above shows that the gain of the KF is chosen to minimize the variance of the error in the estimate. The optimal gain at each step can be iteratively obtained by using Eqs. (10), (12) and (14).

VERIFICATION USING FIELD MONITORING DATA

Instrumented Tsing Ma Bridge (TMB)

The Tsing Ma Bridge (TMB) with a main span of 1,377 m, as shown in Figure 2, is a suspension bridge in Hong Kong carrying both highway and railway traffic. The deck of TMB is a double-deck box with truss stiffening and non-structural edge fairing as illustrated in Figure 3. The longitudinal diagonally braced trusses on north and south sides of the cross-section consist of top chords, diagonal struts and bottom chords. In the longitudinal direction, the bridge deck continuously expands from the Ma Wan abutment to the Tsing Yi abutment. On the Ma Wan abutment, the bridge deck is supported on hinge bearings which allow the rotation of bridge deck other than the displacement; whereas an expansion joint is provided on the Tsing Yi abutment to accommodate the longitudinal displacement of the deck due to temperature variation. The constraint condition of the bridge deck on the internal piers and towers allows free movement of the deck in the longitudinal direction.

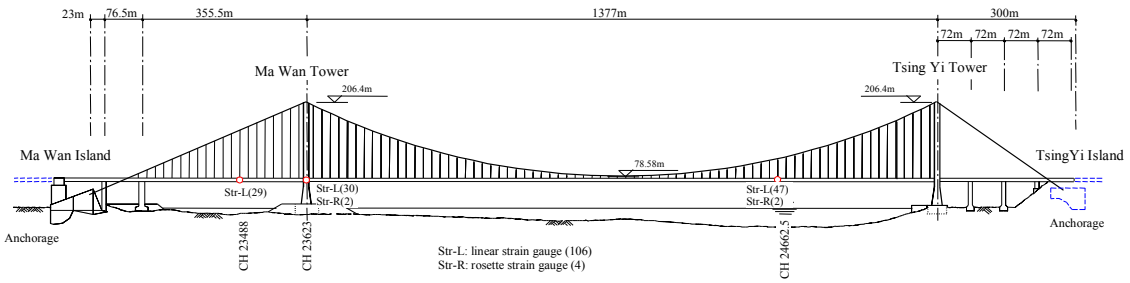

Figure 2 Tsing Ma Bridge and sections instrumented with strain gauges

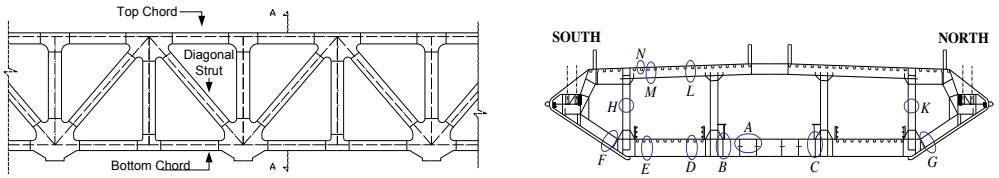

(a) (b)

Figure 3 Deck trusses of TMB: (a) elevation view; (b) cross-section view

As part of a long-term SHM system instrumented on TMB (Wong 2007; Wong and Ni 2011), 110 strain gauges were installed to measure dynamic strain response at three bridge deck sections denoted by CH23488, CH23623 and CH24662.5 (chain mileages of the deck sections of TMB) as shown in Figure 2. The deployment locations of strain gauges include the chord members (top chords, diagonal struts and bottom chords) of the longitudinal trusses, cross-frame chord members, bracing members, deck trough and rocker bearings at one tower. The strain gauges installed on the deck truss members include single, pair and rosette sensors. The strain data were continuously acquired at sampling rates of 25.6 Hz and 51.2 Hz, respectively.

Extraction of Traffic-induced Strain Responses

Figure 4 illustrates typical one-day monitoring data of strain responses of the longitudinal top and bottom chords on deck section CH24662.50 under weak wind condition. It is seen that the magnitude of the strain responses acquired at about 2:00 to 5:00 am is relatively small since railway traffic ceases to operate during this time period. It is also observed that there is a trend ingredient (low-frequency component) in the strain time histories, which is attributed to the daily cycle effect of temperature variation after confirming its synchronism with the longitudinal displacement time history concurrently measured at the expansion joint. The ingredient caused by the temperature effect, although considerably large, contributes little to the stress because the majority of temperature-induced strain is released by movement and rotation of the bridge deck at the expansion joint and bearings.

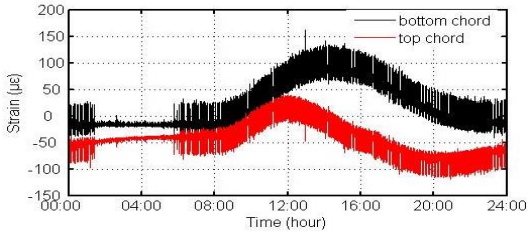

Figure 4 Total strain responses of top and bottom chords on deck section CH24662.5

A multi-component decomposition method (Ni *et al*. 2011), which uses the de-correlation and perfect reconstruction (PR) properties of discrete wavelet transform and embeds a correlation criterion for physical source extraction, has been developed to infer the temperature-induced ingredient from raw measurement data of strain and extract the traffic-induced strain response. Figure 5 shows the extracted traffic-induced strain responses of the longitudinal top and bottom chords on deck section CH24662.50 after eliminating temperature effect. From Figures 4 and 5, it is observed that the measured raw (total) strain responses do not display the flexural behavior owing to the presence of temperature effect. After eliminating temperature effect, the strain responses (which are mainly caused by traffic loading) at the top and bottom chords of the same deck section

evolve with time in almost identical amplitudes but opposite directions, indicating flexural bending behavior of the bridge deck under traffic loading.

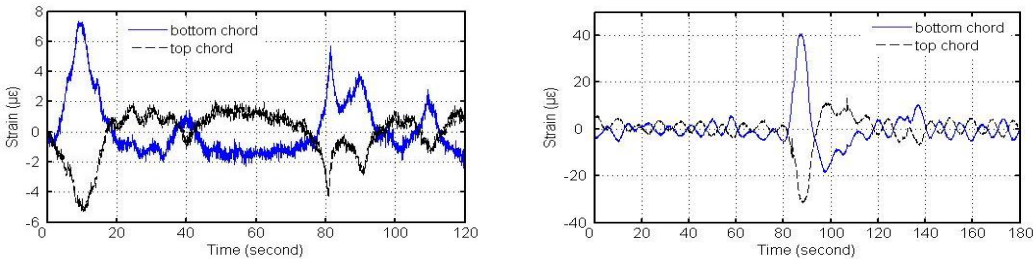

(a) (b)

Figure 5 Traffic-induced strain responses of top and bottom chords on deck section CH24662.5: (a) under highway traffic; (b) under railway traffic

Estimation of Neutral-axis Position under Different Load Patterns

In the absence of damage, the estimated neutral-axis position should be independent of the traffic load patterns. It is testified herein using the field monitoring data from TMB. Figure 6 shows the traffic-induced strain responses experienced by the longitudinal top and bottom chords on deck section CH24662.50 for a typical day (24 hours) under weak wind condition, which are extracted from raw measurement data after eliminating temperature effect. As afore-mentioned, the strain responses acquired during about 2:00 to 5:00 are relatively small because of no railway traffic. It evidences that the strain responses are sensitive to traffic load patterns.

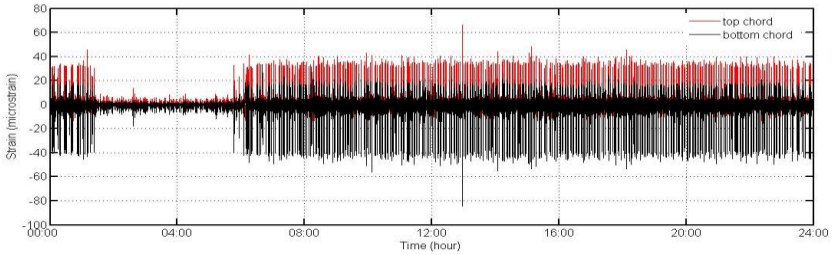

Figure 6 Traffic-induced strain responses experienced by top and bottom chords on deck section CH24662.5 for a typical day

Four segments of the strain response time histories with different traffic load patterns are selected for the present study: (i) 00:00 to 02:00; (ii) 03:00 to 05:00; (iii) 05:00 to 07:00; (iv) 10:00 to 12:00. The KF estimator is executed to estimate the neutral-axis position of the deck section from these four segments of strain data, respectively. Figure 7 shows the traffic-induced strain responses during 00:00 to 02:00 (segment 1), which include a transition of traffic pattern from having to not having railway traffic. Although this transition pattern is remarkably reflected in the strain responses, it does not affect the neutral-axis position estimated by the KF estimator as shown in Figure 8. Figure 9 illustrates the strain response data acquired during 03:00 to 05:00 (segment 2). Because there is no railway traffic in this time period, the magnitude of the strain responses is much lower than other segments, and a relatively low signal-to-noise ratio is expected for this segment of monitoring data. The neutral-axis position estimated by the KF estimator during this time period is shown in Figure 10.

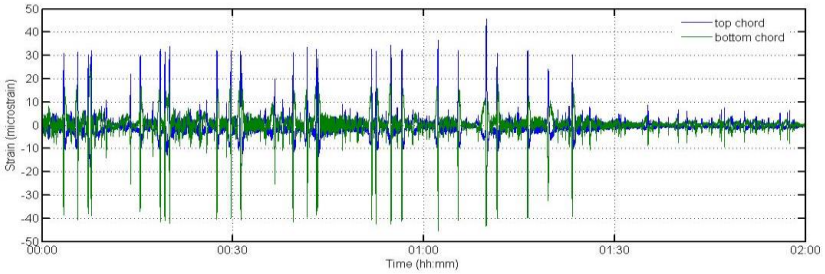

Figure 7 Traffic-induced strain time histories during 00:00 to 02:00

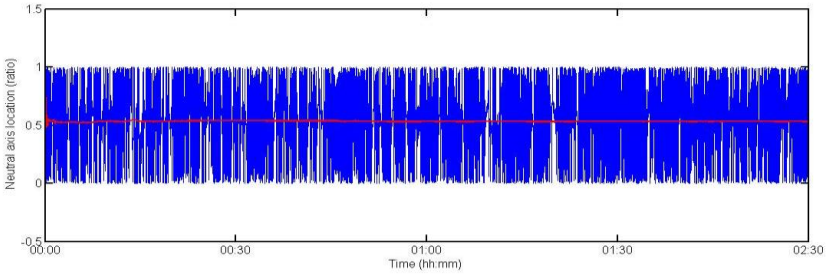

Figure 8 Estimated neutral-axis position from strain data acquired during 00:00 to 02:00

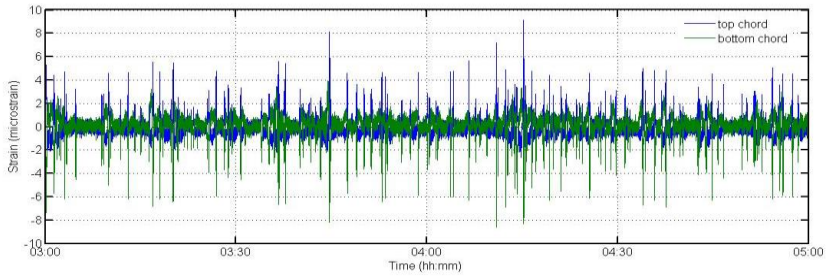

Figure 9 Traffic-induced strain time histories during 03:00 to 05:00

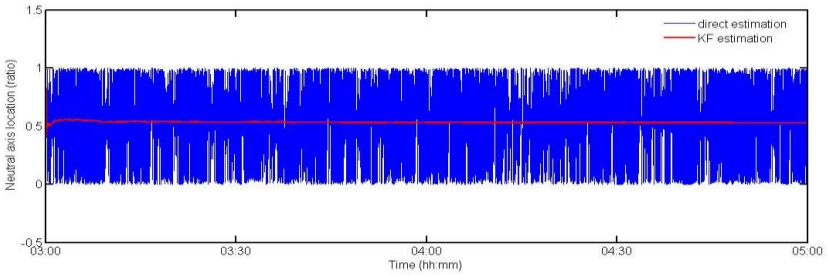

Figure 10 Estimated neutral-axis position from strain data acquired during 03:00 to 05:00

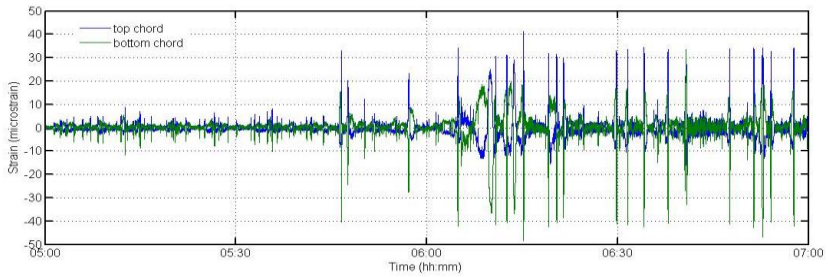

Figure 11 Traffic-induced strain time histories during 05:00 to 07:00

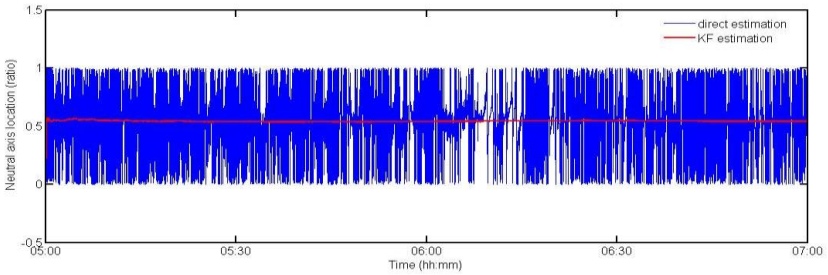

Figure 12 Estimated neutral-axis position from strain data acquired during 05:00 to 07:00

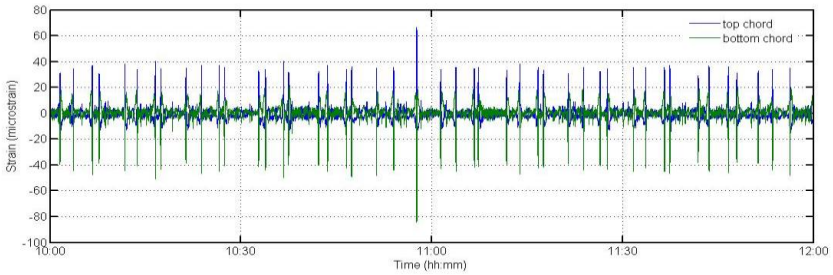

Figure 13 Traffic-induced strain time histories during 10:00 to 12:00

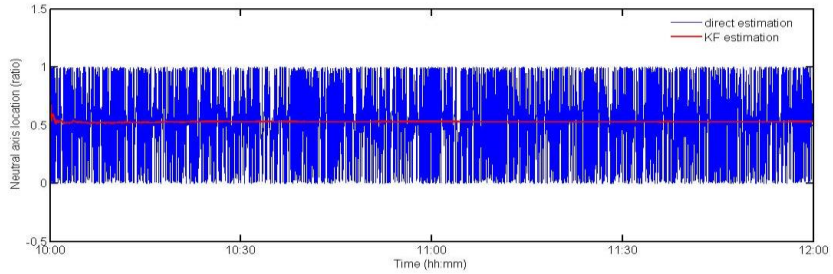

Figure 14 Estimated neutral-axis position from strain data acquired during 10:00 to 12:00

In the time period of 05:00 to 07:00 (segment 3), there is a traffic pattern transition from not having to having railway traffic as shown in Figure 11. Figure 12 illustrates the neutral-axis position estimated by the KF estimator during this time period, which is not affected by the traffic pattern transition. Figure 13 shows the traffic-induced strain responses in the time period of 10:00 to 12:00 (segment 4), where the load pattern is characterized by mixed highway and railway traffic. The estimation results of the neutral-axis position by the KF estimator are illustrated in Figure 14. No observable variation in the estimated neutral-axis position is found.

The estimated neutral-axis position by using the whole-day (24-hour) data is illustrated in Figure 15. It is observed that there are no remarkable transition patterns appearing in the sequence of the estimated neutral-axis position although they do exist in the strain response time histories. Table 1 summarizes the estimated values of the neutral-axis position when using different segments of strain monitoring data. The estimated neutral-axis position ranges from 0.5408047 to 0.5476296 (-0.49% to 0.77% of the mean value) under different traffic load patterns (highway traffic, railway traffic, and their combination). It is concluded that the proposed KF estimator can achieve consistent and robust estimation of the neutral-axis position using strain monitoring data obtained under different traffic load patterns. The application of using the estimated neutral-axis position for damage detection of bridge deck is addressed elsewhere (Xia 2011).

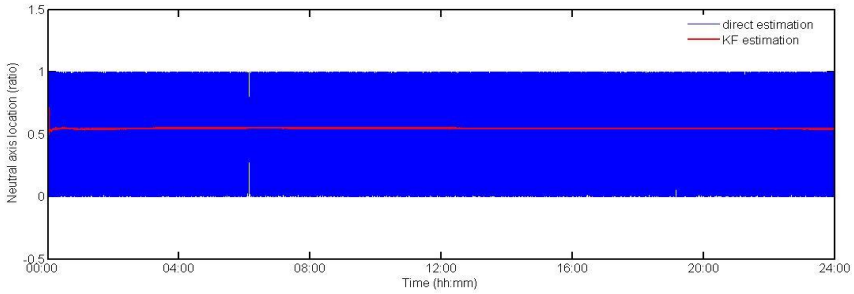

Figure 15 Estimated neutral-axis position from strain data acquired during 00:00 to 24:00

Table 1 Estimated neutral-axis position in ratio under different traffic load patterns

Time period	Estimated neutral-axis position in ratio
00:00 to 02:00	0.5423849
03:00 to 05:00	0.5476295
05:00 to 07:00	0.5425693
10:00 to 12:00	0.5408047
00:00 to 24:00	0.5438627

CONCLUSIONS

Because of its high sensitivity to local damage, the neutral-axis position estimated from strain responses under traffic loading has been considered as a damage indicator for bridge deck assessment. However, the presence of measurement noise and varying traffic load patterns might significantly affect the accuracy of neutral-axis position estimation. In this study, a KF estimator was formulated to locate the neutral-axis position of bridge deck from measured strain responses under traffic loading. Its capability for consistently locating the neutral-axis position under varying traffic load patterns was verified using the field monitoring data from the instrumented TMB. The field monitoring data from TMB evidences the flexural bending behavior of the bridge deck under traffic loading. The validation study using the field monitoring data shows that the estimated neutral-axis position from the traffic-induced strain response data of TMB remains almost unchanged under different traffic environments (highway traffic, railway traffic, and their combination), verifying the robustness of the proposed KF estimator to varying traffic loading and the independence of the neutral-axis position on traffic load patterns.

ACKNOWLEDGMENTS

The work described in this paper was supported by a grant from the Research Grants Council of the Hong Kong Special Administrative Region, China (Project No. PolyU 5224/13E).

REFERENCES

Adewuyi, A.P., Wu, Z. and Serker, N.H.M.K. (2009), "Assessment of vibration-based damage identification methods using displacement and distributed strain measurement". *Structural Health Monitoring*, 8(6), 443-461.

Aktan, A.E., Chase, S., Inman, D. and Pines, D. (2001). "Monitoring and managing the health of infrastructure systems". In: S.B. Chase, A.E. Aktan, eds., *Health Monitoring and Management of Civil Infrastructure Systems*, Proceedings of SPIE Vol. 4337, SPIE, Bellingham, Washington, USA (CD-ROM).

Ansari, F. (2009). "Fiber optic sensors for structural health monitoring of civil infrastructure systems". In: V.M. Karbhari, F. Ansari, eds., *Structural Health Monitoring of Civil Infrastructure Systems*, Woodhead Publishing, Cambridge, UK, 260-282.

Bao, X. and Chen, L. (2011). "Recent progress in Brillouin scattering based fiber sensors". *Sensors*, 11(4), 4152-4187.

Bastianini, F., Matta, F., Rizzo, A., Galati, N. and Nanni, A. (2007). "Overview of recent bridge monitoring applications using distributed Brillouin fiber optic sensors". *Journal of Nondestructive Test*, 12(9), 269-276.

Brown, R.G. and Hwang, P.Y.C. (1997). *Introduction to Random Signals and Applied Kalman Filtering*, 3rd Edition, John Wiley & Sons, New York, USA.

Catbas, F.N. and Aktan, A.E. (2002). "Condition and damage assessment: issues and some promising indices". *ASCE Journal of Structural Engineering*, 128(8), 1026-1036.

Cardini, A.J. and DeWolf, J.T. (2009). "Long-term structural health monitoring of a multi-girder steel composite bridge using strain data". *Structural Health Monitoring*, 8(1), 47-58.

Chakraborty, S. and DeWolf, J.T. (2006). "Development and implementation of a continuous strain monitoring system on a multi-girder composite steel bridge". *ASCE Journal of Bridge Engineering*, 11(6), 753-762.

Fujino, Y., Siringoringo, D.M. and Abe, M. (2009). "The needs for advanced sensor technologies in risk assessment of civil infrastructures". *Smart Structures and Systems*, 5(2), 173-191.

Glišić, B. and Inaudi, D. (2007), *Fibre Optic Methods for Structural Health Monitoring*, John Wiley & Sons, Chichester, UK.

Kalman, R.E. (1960). "A new approach to linear filtering and prediction problems". *ASME Journal of Basic Engineering*, 82(1), 35-45.

Ko, J.M. and Ni, Y.Q. (2005). "Technology developments in structural health monitoring of large-scale bridges". *Engineering Structures*, 27(12), 1715-1725.

Li, H.N., Li, D.S. and Song, G.B. (2004). "Recent applications of fiber optic sensors to health monitoring in civil engineering". *Engineering Structures*, 26(11), 1647-1657.

Liu, M., Frangopol, D.M. and Kim, S. (2009). "Bridge safety evaluation based on monitored live load effects". *ASCE Journal of Bridge Engineering*, 14(4), 257-269.

Mufti, A.A. (2002). “Structural health monitoring of innovative Canadian civil engineering structures”. *Structural Health Monitoring*, 1(1), 89-103.

National Transportation Safety Board (NTSB) (2008), “Collapse of I-35W Highway Bridge, Minneapolis, Minnesota, August 1, 2007”. *Highway Accident Report No*. *NTSB/HAR-08/03*, Washington DC, USA.

Ni, Y.Q., Wong, K.Y. and Xia, Y. (2011). “Health checks through landmark bridges to sky-high structures”. *Advances in Structural Engineering*, 14(1), 103-119.

Ni, Y.Q., Xia, H.W., Wong, K.Y. and Ko, J.M. (2012). “In-service condition assessment of bridge deck using long-term monitoring data of strain response”. *ASCE Journal of Bridge Engineering*, 17(6), 876-885.

Wang, M.L. and Yim, J. (2010). “Sensor enriched infrastructure system”. *Smart Structures and Systems*, 6(3), 309-333.

Wong, K.Y. (2007). “Design of a structural health monitoring system for long-span bridges”. *Structure and Infrastructure Engineering*, 3(2), 169-185.

Wong, K.Y. and Ni, Y.Q. (2011). “Structural health monitoring of a suspension bridge”. In: B. Bakht, A.A. Mufti, L.D. Wegner, eds., *Monitoring Technologies for Bridge Management*, Multi-Science Publishing, Essex, UK, 365-390.

Wu, Z.S., Xu, B., Takahashi, T. and Harada, T. (2008). “Performance of a BOTDR optical fibre sensing technique for crack detection in concrete structures”. *Structure and Infrastructure Engineering*, 4(4), 311-323.

Xia, H.W. (2011). *SHM-based Condition Assessment of In-service Bridge Structures Using Strain Measurement*, PhD Thesis, Department of Civil and Structural Engineering, The Hong Kong Polytechnic University, Hong Kong.

Xia, H.W., Ni, Y.Q., Wong, K.Y. and Ko, J.M. (2012). “Reliability-based condition assessment of in-service bridges using mixture distribution models”. *Computers and Structures*, 106-107, 204-213.